

Electronic Supporting Information (ESI)

A planar impedance sensor for 3D spheroids

V. F. Curto^{a§}, M. P. Ferro^{a§}, F. Mariani^b, E. Scavetta^b, R. M. Owens^{a,†}

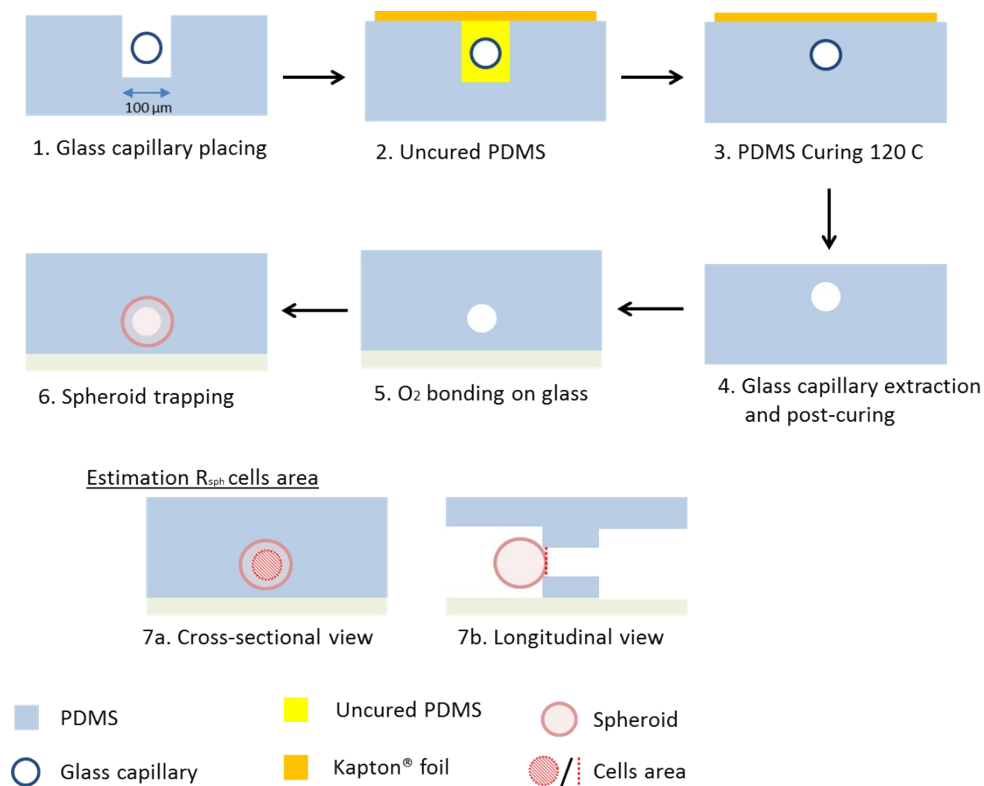


Figure S1. Circular-shaped microtrap fabrication schematics. (1) A glass capillary (outer diameter 80 μm) was carefully placed inside the PDMS squared bottle neck trap (width 100 μm , height 225 μm). (2) A 125 μm thin foil of polyimide was positioned on top in order to provide a reversible seal of the straight half of the microtrap device. The polyimide foil was fixed in position using polyimide tape. (3) A small drop of uncured PDMS was allowed to flow by capillarity inside the microchannel in order to fill the gaps in between the cured PDMS microtrap and the glass capillary. The microtrap was then placed in an oven pre-heated at 120°C for 2 minutes in order to achieve a fast curing rate of the PDMS around the glass capillary. (4) The glass capillary was gently pulled out from the trap and the thin polyimide foil removed. The PDMS microtrap device was then fully cured for 2 hours at 80°C. Finally, inlet and outlet ports were punched in the PDMS and both microtrap and OECT device were plasma activated to obtain irreversible sealing of the microtrap device with the planar OECT. (*bottom*) Schematic representation of the cells area used to calculate the spheroid resistance (R_{sph}) in $\Omega\cdot\text{cm}^2$.

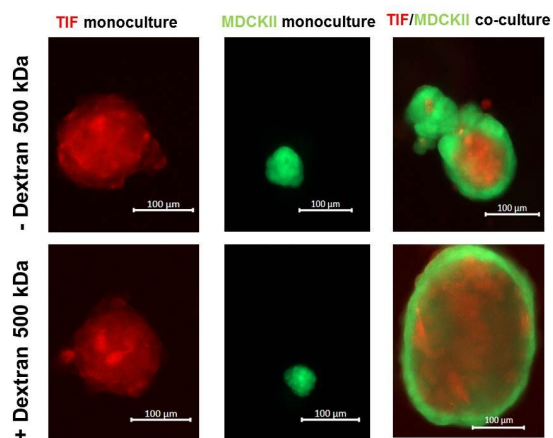


Figure S2. Mono-culture of TIF pLifeAct and MDCKII eGFP spheroids and co-culture TIF pLifeAct/MDCK II eGFP spheroids formed in the absence (-) and presence (+) of 3,83 mg/ml dextran (500kDa) in the culture media. Significant improvements in spheroid circularity were observed for the co-culture system.

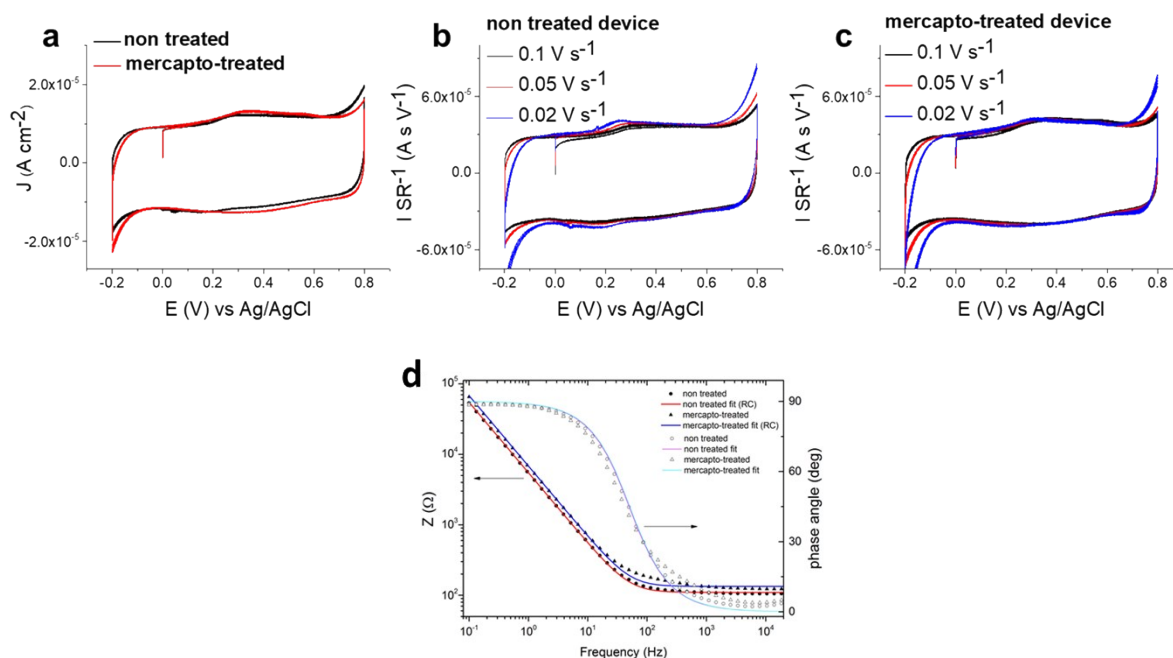


Figure S3. Electrochemical characterisation of non-treated vs mercapto-treated PEDOT:PSS electrodes in 100 mM NaCl. Electrochemical characterization was carried out using a standard three electrode electrochemical cell with a PEDOT:PSS working electrode, Ag/AgCl as the reference electrode and a Pt wire as counter electrode. a) Comparison of the Cyclic Voltammograms at 0.05 V s^{-1} for the non-treated and mercapto-treated electrodes. b) and c) Cyclic voltammograms recorded at different scan rates for a non-treated and a mercapto-treated sample, respectively. In all cases, comparable and typically capacitive behaviour ascribed to PEDOT was found to be unchanged in the presence and absence of the mercapto layer on gold. d) Impedance bode and phase angle plots for the non-treated and mercapto-treated electrodes showing unaffected electrode-electrolyte interface features. Data fitting was performed using an R_sC_p (resistor and capacitor) equivalent circuit, where C_p accounts for polymer capacitance and R_s represents electrolyte resistance.

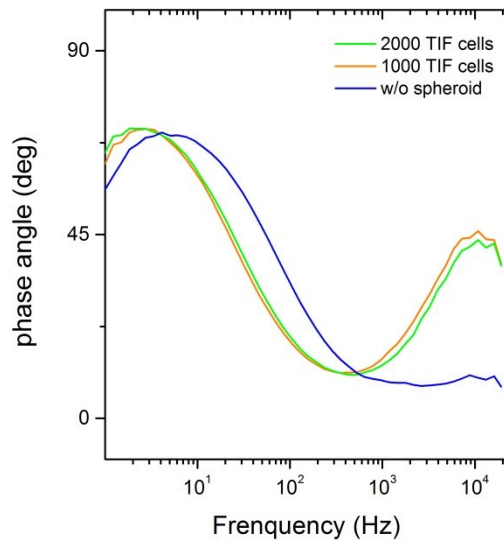


Figure S4. Phase angle plot of the impedance spectra shown in Figure 3c measured in the presence (green – 2000 cells; orange – 1000 cells) and absence (blue) of TIF spheroids inside the circular-shaped trap.

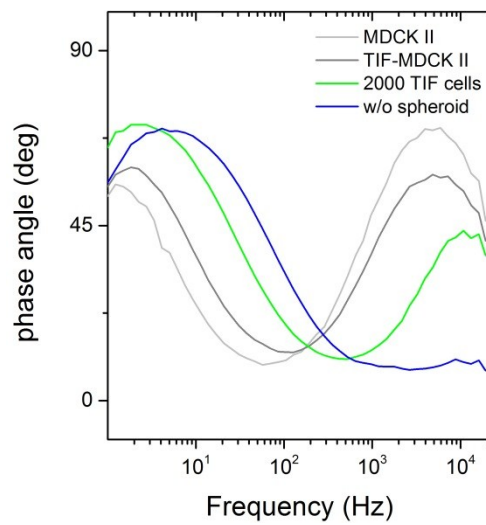


Figure S5. Phase angle plot of the impedance spectra shown in Fig.4d measured in the presence of a MDCK II spheroid (light grey) and TIF/MDCK II spheroid (dark grey) inside the circular-shaped trap.

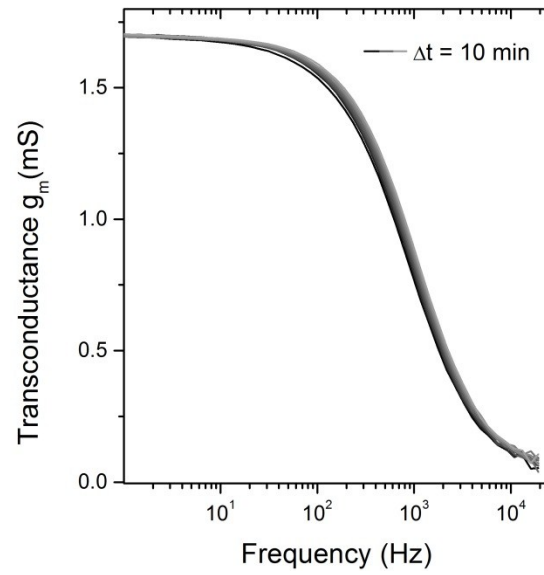


Figure S6. Over time measurements of the frequency dependent response of the organic electrochemical transistor in the presence of triton X-100 ($170\mu\text{M}$) dissolved in cell culture media. A measurement was performed every 10 minutes, sequentially from black curve ($t=0$ min) to light grey curve ($t=130$ min).